Received: 13 May 2023 | *Revised:* 12 July 2023 | *Accepted:* 19 July 2023
DOI: 10.37917/ijeee.20.1.13 *Vol. 20 | Issue 1 | June 2024*

Iraqi Journal for Electrical and Electronic Engineering
Review Article

Open Access
IJEEE University of Basrah College of Engineering

A Review of Design and Modeling of Pneumatic Artificial Muscle

Wafaa Al-Mayahi*, Hassanin Al-Fahaam
Department of Computer Engineering, University of Basrah, Basrah, Iraq

Correspondance
*Wafaa Al-Mayahi
Department of Computer Engineering,
University of Basrah, Basrah, Iraq
Email: engpg.wafaa.daraj@uobasrah.edu.iq

Abstract
Soft robots, which are often considered safer than rigid robots when interacting with humans due to the reduced risk of injury, have found utility in various medical and industrial fields. Pneumatic artificial muscles (PAMs), one of the most widely used soft actuators, have proven their efficiency in numerous applications, including prosthetic and rehabilitation robots. PAMs are lightweight, responsive, precise, and capable of delivering a high force-to-weight ratio. Their structure comprises a flexible, inflatable membrane reinforced with fibrous twine and fitted with gas-sealing fittings. For the optimal design and integration of these into control systems, it is crucial to develop mathematical models that accurately represent their functioning mechanisms. This paper introduces a general concept of PAM's construction, its various types, and operational mechanisms, along with its key benefits and drawbacks, and also reviews the most common modeling techniques for PAM representation. Most models are grounded in PAM architecture, aiming to calculate the actuator's force across its full axis by correlating pressure, length, and other parameters that influence actuator strength.

Keywords
Soft Actuator, Pneumatic Artificial Muscle, McKibben Muscle, Modeling.

I. Introduction

Many different types of creatures and plants use soft structures without any rigid parts to perform intricate movements. Muscle hydrostats, such as octopus arms and elephant trunks, are almost entirely made up of muscle and connective tissue. Plant cells can also alter shape via osmosis without the requirement for a rigid skeletal structure. Inspired by these creatures and plants, scientists create and construct robots with soft industrial actuators that don't have hard skeletons. These robots are commonly known as soft robots. One of the most famous soft actuators is PAM [1, 2], also renowned as the McKibben pneumatic muscle [3], fluid actuator [4], fluid-driven tension actuator [5], fluid artificial muscle (FAM), or the biomimetic actuator. PAMs are used in electronic robotics, anthropomorphic and humanoid robotics, physical therapy and rehabilitation robotics [6–8], and industrial process mechanization [9]. It was invented by Joseph L. McKibben [10, 11] and utilized by polio patients as an orthopedic tool. The McKibben device was initially utilized as a pneumatic actuator in combination with standard pneumatic cylinders [12, 13]. There are three main types of PAM: non-fiber-reinforced [14], straight-type fiber-reinforced [15] and braided fiber-reinforced [16]. The McKibben muscle belongs to the fiber-braided PAM which is the most common type. It is possible to divide muscles into the following four types: embedded muscle, pleated muscle, netted muscle, and braided muscle [17].

Gaylord was the first who described a model for PAM mechanics and defined it as an extended tubular medium bounded by a woven sheath that forms an extended chamber that contracted in length when expanded circumferentially [4]. PAMs are very light actuators that respond quickly, smoothly, and accurately [18, 19], in addition to being capable of producing great force when fully extended [10, 20]. These muscles are made of pure rubber surrounded by a double-braided helical wire

that contract when radially stretched. The building material consists simply of a flexible, inflatable membrane reinforced with fibrous twine and has gas-sealing fittings to bear a mechanical load at one end. When the membrane is compressed, there is an expansion in the radial direction, while there is a contraction in the axial direction along its length. This axial contraction is the mean by which PAM applies a pulling force on its final effects [13, 21, 22].

Soft robots are an excellent substitute for rigid robots, which may cause a risk of injury when these machines are used for humans. Robots made of soft materials are safer in the event of any eventuality, including control failures, human mistakes, or any unforeseen malfunction of the robot arm itself [23–25]. Due to its lots of benefits including its lightweight [26], low power to weight ratio, high strength-to-weight ratio [27, 28] (PAMs have a lifting force of 6000 N despite weighing just roughly 800 grams (and high strength relative to volume, which is five times greater than that provided by electric motors [29], the ability to be molded into various shapes, there is no mechanical wear due to the absence of mechanical parts [30, 31], simple structures, low cost [32, 33] as PAM can be manufactured from inexpensive materials for sale, use of readily available compressed air, with high degrees of freedom due to the soft actuator's ability to bend [34–36], it is more secure than other devices that make use of electricity, heat, or chemically active materials [2, 10, 11, 13].

Despite these advantages, PAMs also have several disadvantages that may limit their application. The friction between the wires of the braided sleeve causes hysteretic behavior in the majority of these PAMs. They also suffer from nonlinear behavior due to the compressibility of the air inside it and the inner tubes viscoelastic characteristics, and the geometrically complicated behaviors of the outer covering of the PAM [37–39]. The produced force and the operating pressure threshold to develop the muscle are affected by the stiffness of the rubber as well as the material used. Rubber fatigue failure was identified by Klute and Hannaford as the most typical failure of muscles. In addition to these drawbacks, the main trouble with muscles is displacement limitation [29, 40].
Various models have been suggested to define the behaviors of PAM, most of which depend on the cylindrical shape after deformation. Many researchers have focused on miniaturized versions of PAM utilized in a variety of applications, including cardiac compression devices and wearable exoskeletons. [41, 42] .
In addition to the McKibben muscle, other types of PAM have been developed, such as the rubbertuator made by the Bridgestone company, the air muscle made by the Shadow Robot Company, fluidic muscle made by the Festo company, PPAM (pleated pneumatic artificial muscles) developed by the Vrije University of Brussels, ROMAC (RObotic Muscle ACtuator), Netted muscles like Yarlott, Kukolj, PAM reinforced by straight glass fiber, Embedded muscles like Morin muscle, Bladwin muscle, Paynter Hyperboloid Muscle, Kleinwachter, and Sleeved Bladder Muscle [43, 44]. Fig. 1 shows some of the pneumatic muscle types.

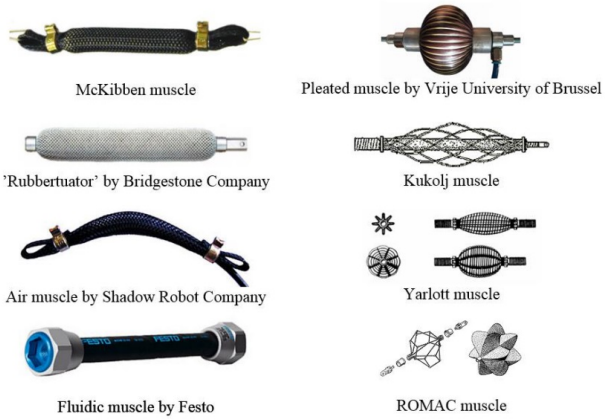

Fig. 1. Different types of pneumatic muscles [44].

The arrangement of this paper is as follows. It provides an overview of the structure and functioning of the PAM, and how the muscle's formation is impacted by the structure that produces either an extensor muscle or a contractor muscle. After that, introduces various models of PAM, beginning with the Geometrical model formulated using mathematical equations. It is presented for different types of muscles (contraction and extension PAM, bidirectional PAM, bending-contraction, and bending-extension PAM) followed by the Phenomenological model of PAM and the Empirical model, and finally, conclusions are presented.

II. Construction and Operation of PAM

PAM is an actuator that functions extremely similar to a human muscle. It contracts through thickening. Pumping high-pressure air through the rubber tube causes it to inflate like a balloon. PAMs are dramatically different from traditional pneumatic actuators. The most common pneumatic muscle design is based on the McKibben muscle. PAM is made up of a rubbery inner bladder bounded by a braided sleeve, one end of the muscle's tube is connected with the source of air pressure and the opposite end is tightly sealed to prevent air leakage [1,45,46]. When the actuator is compressed, its length changes linearly. Depending on how the muscle is built, it will either contract to form the Contraction muscle (CPAM)

or stretch to form the extension muscle (EPAM) [23]. When air exits from the tube, the interior mesh functions as a spring to return the tube to its original shape [47].
The maximum diameter of the nylon sheath expands with a reduction in length, where the expansion of the air muscle causes the inner tube to thicken up to a certain limit. After this point, each additional pressure increase causes the PAM to contract, thereby reducing the length of the nylon sheath [45] and thus applying a pulling force on its load. The force and motion produced by this kind of actuator are unidirectional and linear [4] .
Muscles can be manufactured in different sizes and lengths to produce a different output force. Lengths of muscles range from fewer than 10 cm to 400 cm, while the range of the diameters from less than 10 mm to 70 mm [30][30]. If the braiding angle is less than 54.7 degrees, PAM functions as a contraction actuator. If the angle is greater than 54.7 degrees, it acts as an extension actuator, which has the braided sleeve length sufficiently more than the inner rubber tube length. Additionally, the proportion of contraction varies from muscle to muscle but not exceeds 35% [30]. Also, the amount of extension varies from one muscle to another, but it is not less than 50% [48]. The force created by PAM depends on the air pressure, the muscle initial length, the degree of shortening, and the material qualities [49, 50].
Because this type of actuator becomes more popular, several different types of PAMs have been described in the scientific literature that have different mechanical designs and mathematical models explaining their main process [4].

III. PAM Modeling

There are different types of PAM modeling to predict its nonlinear behavior: Geometrical Model, Phenomenological Model, and Empirical Model.

A. Geometrical Model of PAM

In recent years, different modeling techniques have been introduced in the field of science for modeling PAMs. Although these modeling methods involve a basic and more detailed analysis of PAMs, in the field of PAM applications, most models are based on PAM architecture. The goal of these models is to relate the pressure and the actuator's length to the force it exerts along its entire axis. To get a proper PAM model, variables such as pulling force, the length of the actuator, the pressure of the air, diameter, and material properties play an important role in the dynamic performance of PAM and that explains the reason mathematical models attempt to explain the relationships between these variables. Understanding these relationships is essential in every application consisting of PAMs, particularly if the main goal is to govern their total function [31, 51].
Because it was difficult to directly measure the effect of the braid elasticity, the majority of geometric models assumed that the braid cannot extend to facilitate formulation, despite the significant influence of flexibility of the braid on the geometry and force of the muscle [52]. The PAM force output was modeled using two methods. The first approach relied on energy conservation in the system; no energy is stored in the system elastic walls, zero thickness, and cylindrical shape is retained. The second approach used a detailed analysis of the force [53, 54].

1) Contraction and Extension PAM Models

Gaylord [55] invented the oldest mathematical model to describe and analyze PAM, which assumed that the initial shape of PAM remained cylindrical shape even after deformation. Although expansion would be non-regular, as one end is closed and the other is connected to a source of pressure, the following equations describe the force (F) produced by the kinetic system with length (L), the diameter of the sheath (D), the angle between a braided thread and the cylinder long axis (θ), length of thread (b), and relative pressure ($\hat{P}$) (the difference between absolute internal air pressure and environment pressure).

$$F = \frac{p'\pi D^2}{4}\left(3\cos^2\theta - 1\right) \tag{1}$$

$$\mathrm{L} = \mathrm{b}\cos\theta \tag{2}$$

Schulte and Pearson [56] presented the model which assumes the survival of the cylindrical shape too, and they got the same Gaylord's expression, then developed the model to include the effects of tube elasticity and internal friction as in the equation:

$$\begin{aligned}\mathrm{F} = \tfrac{\pi D^2 P}{4}\left[3\cos^2\gamma - 1\right] + \pi D k_e\Big(\mathrm{L}\sin\gamma - \tfrac{\pi\cos^2\gamma}{\sin\gamma} \\ (\mathrm{D}\sin\gamma - \mathrm{D}_0)\Big) - \pi LDP_c\left(u_s + u_{st}\right)\sin\gamma\end{aligned} \tag{3}$$

Where k_e is the constant of the elasticity of the inner tube found through experiments, L is the length at any value of γ , D_o is the diameter of tubing before inflated, u_s is the coefficient of friction between threads of the sleeve, u_{st} is the coefficient of friction between threads of the sleeve and inner tube. P_c is the differential pressure between P (inflation pressure) and P_i (the pressure desired to inflate the unconstrained inner tube to a diameter equal to the device diameter at any

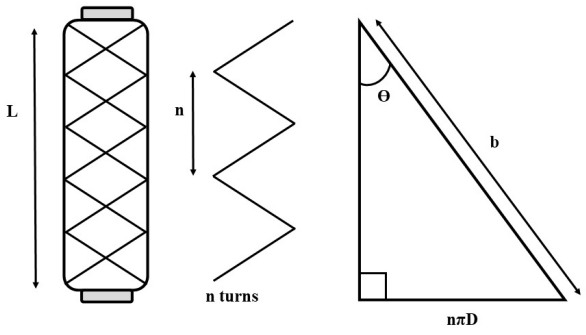

Fig. 2. The parameters of the PAM [1].

value of γ) [57]. Subsequently, many studies were conducted to model the performance and characteristics of these types of actuators, relying on this basic model by adding correction factors, mitigating modeling assumptions, or adding force conditions arising from other phenomena that contribute to PAM physical statistics. Based on the conservation of energy principle, Chou and Hannaford [58, 59] assumed the muscle cylindrical shape in their model and ignored the force of friction between the sleeve and the bladder and the extension of threads in the sleeve. They relied in their model on the geometric parameters of the operator. Fig. 2 shows the relationship between the parameters. The geometric relationship is given by:

$$\mathrm{F} = -P' \frac{dV}{dL} \tag{4}$$

$$\mathrm{V} = \frac{1}{4}\pi \mathrm{D}^2 \, \mathrm{L} \tag{5}$$

$$\mathrm{D} = \frac{b \sin\theta}{n\pi} \tag{6}$$

Where V is cylinder volume and n is the number of turns.

Thus, the tension is linearly proportional to the pressure and is a monotonic function of the braid angle ($0^o < \theta < 90^o$). The maximum amount of shortening will be achieved when $F = 0, i.e.\ \theta = 54.7^o$. Accordingly, they developed their model for expressing force. Taking into consideration the thickness of the shell and the bladder (tk) and the effect of friction between the inner lining and the outer braid, they formulated this friction as a constant force that always opposes the movement of a muscle.

$$\mathrm{V} = \frac{1}{4}\pi (D - 2\mathrm{tk})^2 L \tag{7}$$

$$\mathrm{F} = \frac{P'\pi D^2}{4}\left(3\cos^2\theta - 1\right) + \pi P' \left[D_0 t_k \left(2\sin\theta - \frac{1}{\sin\theta} \right) - t_k^2 \right] \tag{8}$$

Tondu and Lopez [60], Caldwell et al. [61], and Kimura et al. [62] used the law of conservation of energy in the system to design their model. Tondu and Lopez [60] modified Gaylord's basic equation, assuming that the cylinder takes a conical shape after deformation, adding a factor to explain the effects of the non-cylinder side. Thus, the contraction force is represented by the following formula:

$$\mathrm{F}(\varepsilon, P) = \pi r_0^2 \times \mathrm{P}\left[a(1-\varepsilon)^2 - b \right] \tag{9}$$

Where:

$$\varepsilon = \frac{I_0 - I}{I_0},\ 0 \le \varepsilon \le \varepsilon_{\max}, a = \frac{3}{\tan^2\theta_0},\ b = \frac{1}{\sin^2\theta_0} \tag{10}$$

Where θ_0 is the initial braided angle of the sleeve, I and I0 are the length of the bladder before and after the deformation respectively, and ε is the contraction ratio.
Tondu and Lopez improve the previous equation, by adding a correction factor (k) to calculate the final deformation. the k value is determined depending on the type of material by which the muscle is made, and the pressure in the muscle.

$$\mathrm{F}(\varepsilon, P) = \pi r_0^2 \times \mathrm{P}\left[a(1-k\varepsilon)^2 - b \right] \tag{11}$$

$$\varepsilon_{\max} = \frac{1}{k}\left(1 - \sqrt{\frac{b}{a}} \right) \tag{12}$$

Caldwell et al. in [63] relied on the approach of the trapezoidal shape formed by the fibers to derive the geometric model as in Fig. 3. if the length of one side of the trapezoidal is l, and α is the braid angle, the length and the diameter of the muscle are given by:

$$\mathrm{L} = 2 * \ \mathrm{A} * l * \cos\alpha \tag{13}$$

$$\mathrm{D} = \mathrm{f} * \sin\alpha \tag{14}$$

Where A is the trapezoids number within the braid length in the x plane, f is the diametric distance parameter that is equal

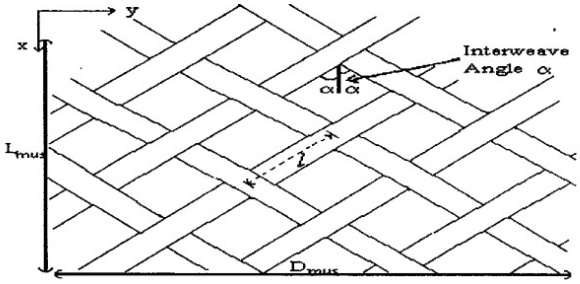

Fig. 3. Trapezoidal muscle braid geometry [63].

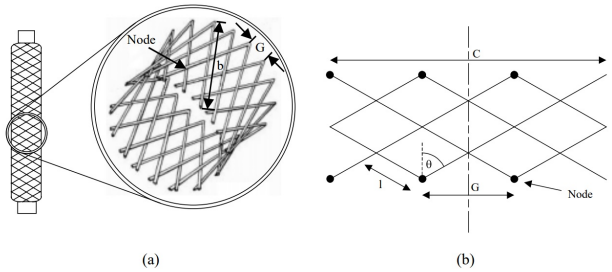

Fig. 4. TShow PAM parameters to calculate the contraction [64].

to $(2Bl)/\pi$, and B is the trapezoids number in the y plane

Davis et al. demonstrated that the main limiting factors to the dynamics of PAM systems are valve resistance and the supply pipe, where resistance is lower when pipes have a large bore, minimum pipe connectors, and large orifice valves. Of note, reducing dead space in the muscle structure to a minimum achieves a peak bandwidth increase of up to 400%. However, various fillers material affect these enhancements [30].

It is worth noting that the muscle reaches a state of stretching where the braid cannot lengthen more or a state of contraction where the braid cannot contract more where the fibers are in close contact with each other so that it prevents further movement [64]. The minimum contraction of PAM is determined by the change in the angle between the braid (θ) which does not exceed 54.7^o [58], that is 30 - 35% of its original length [61,65]. Maximum extension is the minimum angle of the strands and is limited by pushing adjacent strands against each other or when the internal bladder diameter is large to prevent stretching. The minimum strand angle can vary depending on the type of fabric, fiber material, and fiber diameter. The contractile range of the muscle is the difference between its length at the smallest and largest braid angles.

Since this type of muscle cannot have its maximum braid angle changed, the only way to increase its dynamic range is to let it reach a lower braid angle [64]. The minimum strand angle is calculated for a small section of the braid around the circumference of the muscle and the axis is aligned along the actuator, each crossing point being a node. The distance between the nodes will be G, the distance C is the circumference of the muscle, and I is the space between the strands. Fig. 4 shows these parameters.

The value of I is calculated when $\theta = 90^o$. At this point, the equation of the circumference is:

$$\mathrm{C} = 2 * \mathrm{I} * \mathrm{N_c} \tag{15}$$

Where N_c is the number of nodes in one cycle of a muscle circumference.

$$\mathrm{I} = \frac{\pi \cdot D_0}{2 \cdot N_c} \tag{16}$$

$$\mathrm{G} = 2 * \mathrm{I} * \sin\theta \tag{17}$$

$$\theta_{\min} = \frac{\sin^{-1}\left(\frac{D_S \cdot N}{\pi \cdot D_o}\right)}{2} \tag{18}$$

$$\mathrm{L_{max}} = \mathrm{b}\cos\left[\frac{\sin^{-1}\left(\frac{D_s \cdot N}{\pi \cdot D_o}\right)}{2}\right] \tag{19}$$

Doumit and Fahim [54] developed a force-based model that takes into account the netting analysis of the muscle braid and the bladder effect, where it was found that the force-based model is more accurate, but it is more complex compared to the energy model. They used a more realistic geometry by taking into account the irregular shape of the end parts of the muscle during distension, as shown in Fig. 5. The proposed geometry is made of three parts, a conical part for both ends and a cylinder for the middle part of the muscle.

Where L is the total length of the muscle, L_L is the cone's horizontal length, L_z is the length of the cone generator, β is the frustum-cone angle of the muscle ends, L_m is the middle-section length, D is the middle section diameter and d is the end-fixture diameter.

The braid diameter is calculated by:

$$\mathrm{D} = \frac{\sqrt{b^2 - L_m^2}}{\pi n} \tag{20}$$

The diameter of the base of the cone expands during contraction, and the cone horizontal length L_L is:

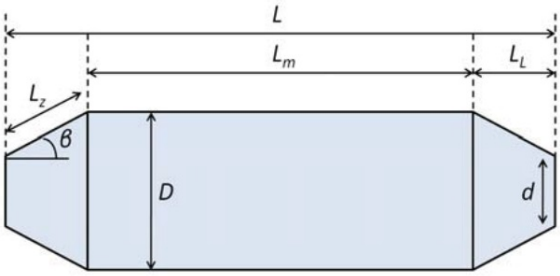

Fig. 5. Geometrical model of PAM [54].

$$L_L = \sqrt{L_z^2 - \left(\frac{D}{2} - \frac{d}{2}\right)^2} \tag{21}$$

The total muscle length (L):

$$\mathrm{L} = L_m + 2L_L \tag{22}$$

If the shape of the muscle is supposed to be cylindrical, the equation for length can be expressed in the following form:

$$\mathrm{L} = \sqrt{b^2 - (\pi n D)^2} \tag{23}$$

Shen and Shi [66] enhanced a mathematical stretching model for PAM which was designed by Festo Company (FMPAM), which is different from McKibben's model, where the elastic material is mixed with the reinforced braided fibers. Muscle length was modeled based on its sigmoid shape in reference [37][37], where muscles of different lengths were used. Ashwin and Ghosal [67] proposed a new model for miniaturized PAM (MPAM) that takes into consideration the bladder's physical properties. They suppose that the primary mode of actuation is contractile to avoid the effect of flexion in the actuator since the derived mathematical models are also valid for the EPAM when comparing the differences in the performance of CPAM and EPAM [68]. It was found that the static properties of MPAMs do not always correspond to the models used in normal-sized PAMs due to the greater proportion between the size taken by the bladder and the internal size of the bladder and the end effects. Hence, several models used to represent MPAM stats require correction factors to be included in the models for larger PAMs. Ashwin also supposed that the shape of PAM remains cylindrical after deformation, the braid thickness can be ignored, and the braid material is inextensible. The expression of the bladder length before the deformation and after deformation are L_0 and L respectively (as shown in Fig. 6), which could be written as:

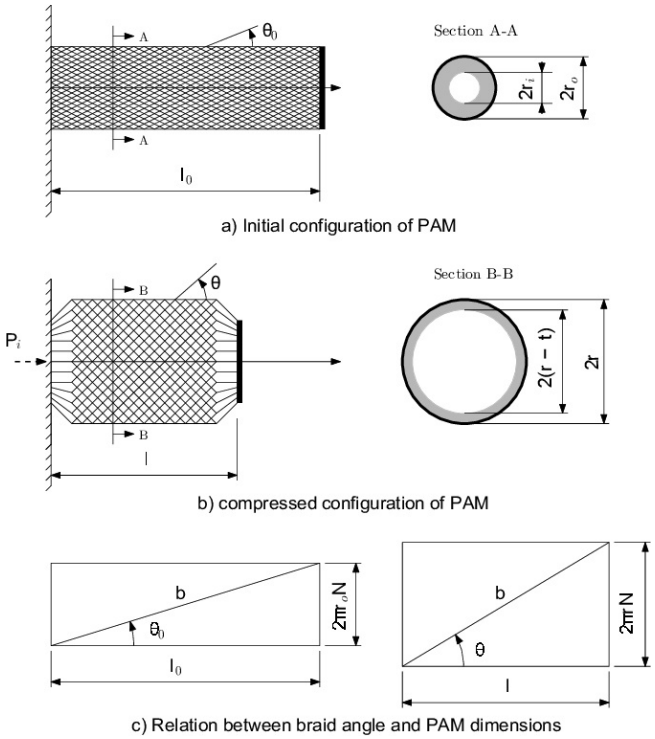

Fig. 6. Nomenclature of MPAM [64].

$$L_0 = \mathrm{b}\cos\theta_0, \quad 2\pi \mathrm{r}_0\,\mathrm{N} = \mathrm{b}\sin\theta_0 \tag{24}$$

$$L = \mathrm{b}\cos\theta, \quad 2\pi \mathrm{r N} = \mathrm{b}\sin\theta \tag{25}$$

Al-Ibadi et al. [69] introduced the correction factor $q(p)$ by multiplying it by the expansion ratio in order to decrease the difference between the experimental and theoretical results. This difference is due to several factors including the non-cylindrical shape of PAM at zero or low pressure supply, no severe contact between the inner rubber tube and the braided sleeve, and the rubber tube resistance.

$$\mathrm{q(p)} = -\left(1 + e^{-0.5p}\right) \tag{26}$$

Najmuddin and Mustaffa [70] conducted several studies to illustrate the effect of the braided mesh and it is used. The mesh with the optimal size leads to the greatest contraction, as it may contract by 51.85% of its original length. In addition, the results demonstrated that an increase in length improves the contraction, whereas an increase in load decreases the contraction as the force remained constant even there is an increase in load due to the constant diameter of the PAM.

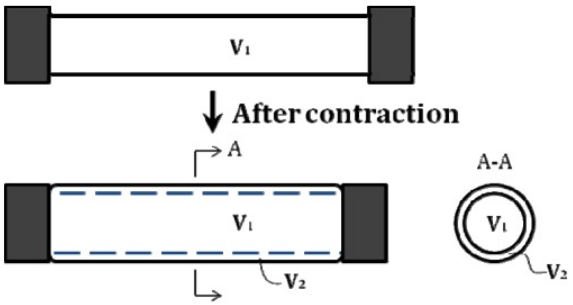

Fig. 7. Divide the muscle's volume into two parts [73]

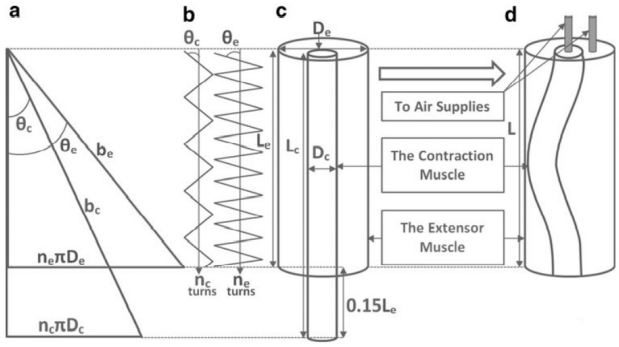

Fig. 8. ECPAM's design [1]

Accordingly, the diameter and length of the bladder are the primary determinants of muscle performance. Li et al. [71] suggested an improved static analysis model for commercially braided PAM that reduces experimentally determined parameters to lower the modeling cost and takes into account irregular shapes close to the final fittings to control for PAM output forces. Several simulations were used to examine the impact of the rubber layer's elastic and frictional forces on the force generated by the air muscle during filling based on the mathematical model that was created [61]. A physics-based static behavior model for PAM was designed considering friction losses between threads, non-cylindrical ends, and the influence of bladder elasticity in order to evaluate the output force and actuator contraction for different applied pressures in the reference [72].

2) Bidirectional PAMs Models

No single muscle can perform both types of motion. Zheng and Shen [73] introduced a new bidirectional muscle model, in which the internal volume of the traditional PAM was separated into two portions that can move in two different directions. Volume (V1) is the volume of a cylinder at the center of the muscle. Its diameter is equal to the diameter of the end connectors of the muscle. Volume (V2) is in the form of a ring surrounding the first volume as in Fig. 7. When a muscle contracts, V1 decreases because it depends on the diameter and length of the muscle, while V2 increases with muscle contraction. The contraction force is the sum of the two forces (the contraction force created by the membrane and the extension force applied to the end connector due to the internal air pressure)

Based on this principle, a solid cylindrical rod or tube was inserted into the muscle. This addition helped to cancel the stretching force and increase the power of the actuator, as it was found that it needs less air to generate the required force (energy consumption decreases by 20% - 37% compared to the identical pneumatic muscle without a rod). Because the two sizes contribute to the production of two opposite forces, the actuator can produce two forces that extend and contract separately. But this design increases the weight of the actuator. Moreover, the stretching force and movement are low compared to the contraction force. Hassan et al. [74] found that it is possible to generate bidirectional motion when changing the angle of the fibers in the braid independently, as the user can change this angle depending on the mechanical adjustment of the actuator. Al-Fahaam et al. [1] design a bidirectional muscle consisting of a CPAM placed within an EPAM where the CPAM is compressed within the bladder of the EPAM (the rubber bladder of the CPAM is 15% longer than the bladder of the EPAM) as illustrated in Fig. 8. Moreover, the muscle formed can change its stiffness without changing its length. The relationship between the length of *CPAM* (L_c) and *EPAM* (L_e) could be represented in the following equation:

$$L_c = 1.15L_e \tag{27}$$

The relationship between the number turns of thread in CPAM (n_c) and in EPAM (n_e), and between the length of a single thread of CPAM sleeve (b_c) and EPAM sleeve (b_e) will be:

$$n_c = 1.15n_e \tag{28}$$

$$2b_c = 1.15b_e \tag{29}$$

The force equation is derived from the calculating equations of the volume, and length of the CPAM with respect to the angle formed by the braided thread and the CPAM central actuator axis (θ_c) will be:

$$F_c = \frac{b_c^2\,(P_c - P_e)}{4\pi n_c^2} \tag{30}$$

Where P_c is the pressure of CPAM and P_e is the pressure EPAM. Thus, the EPAM force equation will be:

$$F_S = \frac{b_c^2 P_e}{4\pi n_c^2}\left(1.15\left(3\cos^2\theta_c - 1\right) - 4\left(3\cos^2\theta_c - 1\right)\right) \quad (31)$$

The total force of the model:

$$F = F_c - F_s = \frac{b_c^2}{4\pi n_c^2}\left(P_c\left(3\cos^2\theta_c - 1\right) + 0.15P_e \left(3\cos^2\theta_c - 1\right) - P_e\left(3\cos^2\theta_e - 1\right)\right) \quad (32)$$

When the muscle is contractor, the value of F is positive, and it is negative in the extensor muscle.

3) Bending-Contraction and Bending-Extension PAMs

Bending PAM has been advanced by many researchers, but most of them focused on Extensor Bending (EB-PAM) because Contraction Bending PAM (CB-PAM) is difficult to achieve [75]. Razif et al. [76] used a two-channel actuator, which is a cylindrical actuator reinforced with spiral fibers around its wall and it has a wall splitting those chambers due to its ability to bend in the right and left direction. When the pressure increases in one chamber, the actuator bends towards the opposite side. Factors such as the thickness of the actuator and partition wall, and the material by which the rubber is made give a large difference in the bending angle when compressed, while the location and materials of the fibers do not show a significant difference in the bending angle. In [77] a pneu network is designed consisting of flexible structures inside which a network of small channels that can be inflated with low pressures. this actuator can bend into a semi-circular shape very quickly and within a short period. Al-Fahaam et al. [23] and Al-Ibadi et al. [69] designed a model of PAM (EBPAM) that can bend where one side is stretched with a thread to prevent stretching, while the opposite side can extended and increase in length when pressed as Fig. 9. The resulting difference in length leads to muscle bending, and the bending angle increases with increasing pressure supplied. The EBPAM analysis depends on an assumption that when the muscle bends, it keeps a circular cross-section, the reinforced side is inextensible, there is no friction between the sleeve threads or between the sleeve and the bladder and the bladder does not have any elastic force [23, 78].

The average length of the actuator is:

$$L_c = (L_o + L_n)/2 \quad (33)$$

Where L_o is the length on the reinforced side and L_n is the length on the free side.

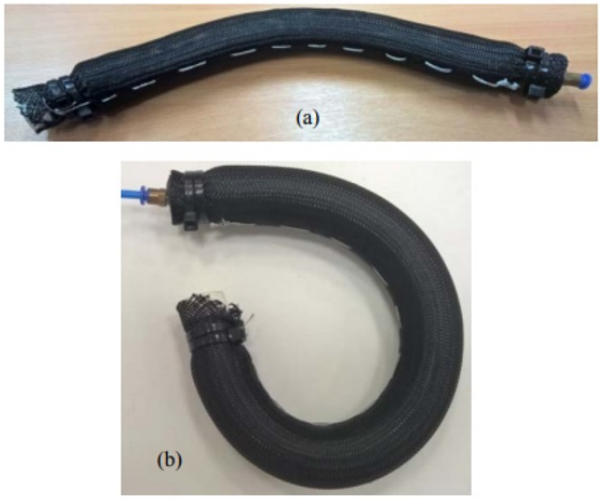

Fig. 9. BE-PAM [69]

The curved actuator diameter is:

$$D_c = r_n - r_o \quad (34)$$

Where r_o is the inner radius and r_n is the outer radius. Fig. 10 explains the geometry of the bending muscle and these parameters. The maximum angle of the thread (θ_{max}) determines the inner radius, which is constant because of the reinforcing thread, and the angle (θ) determines the outer radius and decreases as the muscle bends. The diameter can be computed using the sum of the inner curve's diameter (r_2) and the outer curve's diameter (r_2) as Fig. 11.

$$D_c = r_1 + r_2 = \frac{bsin(\theta) + bsin\theta_{max}}{2n\pi} \quad (35)$$

Taking into account the thickness (t_c) of the bladder and sleeve, the diameter equation will be:

$$D_c = r_1 + r_2 = \frac{bsin(\theta) + bsin\theta_{max}}{2n\pi} - 2t_c \quad (36)$$

The bending angle (α) can be calculated as a function of θ and θ_{max} :

$$\alpha = \frac{bcos(\theta) - bcos\theta_{max}}{D_c} \quad (37)$$

Three muscles were designed with the capacity to extend and bend with multiple degrees of freedom enabling them to reach any position within 360 degrees [79]. A model of the pneumatic soft actuator that couples extensor and contractor muscles was suggested [80]. This actuator can produce changing stiffness in a fixed bending position.

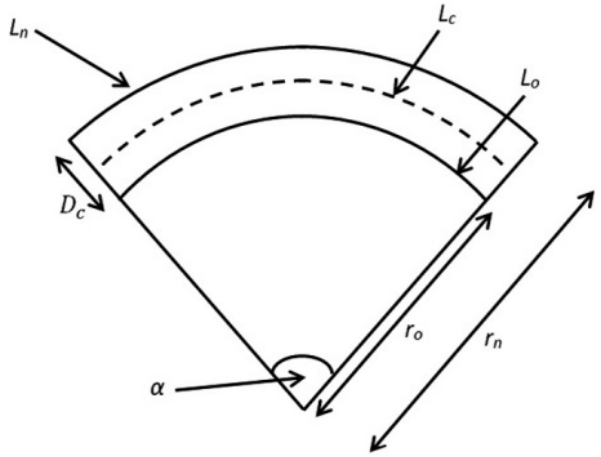

Fig. 10. Muscle geometry during bending [23]

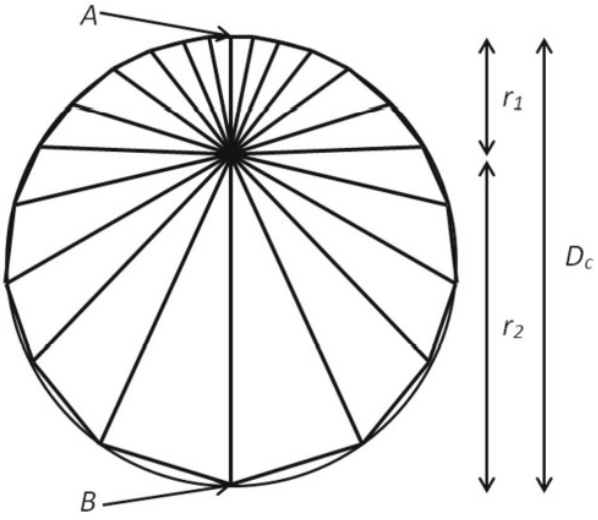

Fig. 11. The diameter inside the bending muscle [23]

From the biological concept of the human body as rigid parts covered by soft tissue, a self-bending contraction actuator (SBCA) is designed in which a flexible rod is inserted between the inner rubber tube and the braided mesh. The rod limits the bending behavior and provides a high load compared to the weight of the actuator. This design can alter the actuator performance by changing the rod size or replacing it [81]. Guan et al. [82] achieved the bending by placing a flexible frame concentrically between the bladder and the braided tubes to restrict the contraction and extension deformation on one side as well as generating a curved deformation towards the reinforced side when inflating. Two models: BE-PAM and BC-PAM were built with symmetric structures. BE-PAM showed greater flexibility and great compliance, but it is more susceptible to deformation under external loads due to its low stiffness, which affects the performance of the gripper built with it. On the other hand, BC-PAM has higher production, more efficiency, higher stiffness, less susceptible to deformation, and its inner frame bears a high-pressure force.
The most important proposed model to describe muscle bending is Chen's model, which consists of two physical models including the beam model and the membrane model. The model indicates that flexibility and internal pressure affect the torque required to bend a muscle [83].

B. Phenomenological Model of PAM

The phenomenological model aims to obtain the best dynamic performance of PAM compared to the static behavior that the geometric models focus on. Colbrunn et al. developed PAM model containing a spring, viscous damper, and Coulomb friction element arranged in parallel [84]. The dynamic model of PAM used by Serres et al. also consists of a spring, a damping element, and a contraction element that are parallel to each other [85] as shown in Fig. 12. The equation describes the phenomenological model for this motion is [86]:

$$M\ddot{y} + B\,\dot{y} + ky = F_{ce} - L \tag{38}$$

Where M is the mass of the moving components, B is the damping coefficient, K is the spring coefficient, F_{ce} is the contractile force coefficient of PAM which acts throughout an entire contraction for a given pressure and L is the external load. In this model, other studies have been conducted such as [87].

C. Empirical Model of PAM

PAM is similar in its mechanical behavior to the spring, as both produce a tensile force when attached to a load. Wickramatunge and Leephakpreeda [88] present an empirical model

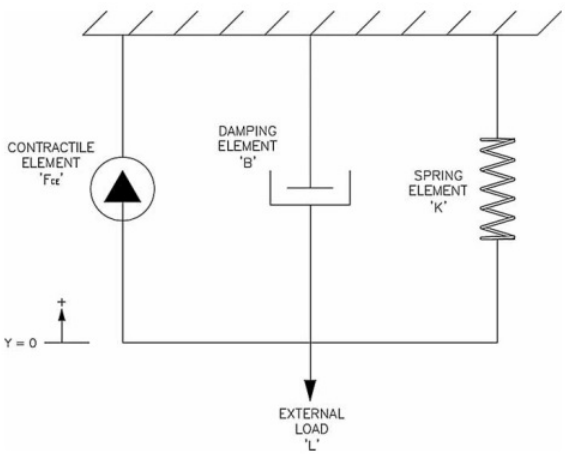

Fig. 12. Phenomenological model [86]

to understand the dynamic behavior of PAM. The experimental results that were conducted showed that physical variables affect the stiffness and strength of PAM. Wickramatunge et al. [89] conducted a study on three different sizes of PAM to understand their mechanical behavior. The results showed the non-linear relationship between contraction as well as air pressure within the muscle and the pull force of PAM. The stiffness does not merely depend on the extended length but also on the air pressure inside the muscle where the compressed air control can be used to adjust the stiffness modulus of the PAM. It was also found that a longer PAM produces a larger working range of motion. A larger diameter PAM is suitable for applying higher force rather than a smaller diameter of the same length.

Ranjan et al. conducted their practical and theoretical experiments on the effect of pressure change on muscle contraction at different loads. the results showed that the contraction increases with the increase in the trapped volume [45]. The contraction range can also be increased by 7% with a contraction force of 16% when the threads used to create the braided sleeve are halved [64]. Hoque et al. [90] tested how the material characteristics such as stiffness and diameter of the bladder affected the performance of PAM actuators.

IV. Conclusion

PAM is an actuator that functions strikingly similar to a human muscle. By pumping high-pressure air through a rubber tube, it inflates like a balloon, leading to a shortening of the muscle by up to 35% or an extension by up to 50% of its length. PAMs differ significantly from traditional pneumatic actuators, with the most popular pneumatic muscle design based on the McKibben muscle. Muscles can be manufactured in varying sizes and lengths, directly influencing the output force. The force generated by an air muscle is contingent upon the pressure of the air, the muscle's initial length and degree of shortening, as well as the material properties. PAM's nonlinear behavior can be predicted using different types of modeling, such as geometrical, phenomenological, and empirical models. This article presented various models for studying the geometric modeling of PAM. It began with the model put forth by Gaylord, which is the oldest mathematical model for describing and analyzing PAM. Subsequently, models describing contraction, extension, bidirectional muscle movement, and muscle bending were also discussed. Moreover, an overview of muscles' construction, function, benefits, and drawbacks was provided.

Conflict of Interest

The authors have no conflict of interest relevant to this research.

References

[1] H. Al-Fahaam, S. Nefti-Meziani, T. Theodoridis, and S. Davis, "The design and mathematical model of a novel variable stiffness extensor-contractor pneumatic artificial muscle," *Soft robotics*, vol. 5, no. 5, pp. 576–591, 2018.

[2] A. Al-Ibadi, K. A. Abbas, M. Al-Atwani, and H. Al-Fahaam, "Design, implementation, and kinematics of a twisting robot continuum arm inspired by human forearm movements," *Robotics*, vol. 11, no. 3, p. 55, 2022.

[3] G. K. Klute and B. Hannaford, "Accounting for elastic energy storage in mckibben artificial muscle actuators," *J. Dyn. Sys., Meas., Control*, vol. 122, no. 2, pp. 386–388, 2000.

[4] F. Daerden, D. Lefeber, *et al.*, "Pneumatic artificial muscles: actuators for robotics and automation," *European journal of mechanical and environmental engineering*, vol. 47, no. 1, pp. 11–21, 2002.

[5] H. M. Paynter, "Hyperboloid of revolution fluid-driven tension actuators and method of making," 1988. US Patent 4,721,030.

[6] H. Majidi Fard Vatan, S. Nefti-Meziani, S. Davis, Z. Saffari, and H. El-Hussieny, "A review: A comprehensive review of soft and rigid wearable rehabilitation and assistive devices with a focus on the shoulder joint," *Journal of Intelligent & Robotic Systems*, vol. 102, pp. 1–24, 2021.

[7] Y. Wang and Q. Xu, "Design and testing of a soft parallel robot based on pneumatic artificial muscles for wrist rehabilitation," *Scientific Reports*, vol. 11, no. 1, p. 1273, 2021.

[8] D. Dragone, L. Randazzini, A. Capace, F. Nesci, C. Cosentino, F. Amato, E. De Momi, R. Colao, L. Masia, and A. Merola, "Design, computational modelling and experimental characterization of bistable hybrid soft actuators for a controllable-compliance joint of an exoskeleton rehabilitation robot," in *Actuators*, vol. 11, p. 32, MDPI, 2022.

[9] J. E. Takosoglu, P. A. Laski, S. Blasiak, G. Bracha, and D. Pietrala, "Determining the static characteristics of pneumatic muscles," *Measurement and Control*, vol. 49, no. 2, pp. 62–71, 2016.

[10] G. Andrikopoulos, G. Nikolakopoulos, and S. Manesis, "A survey on applications of pneumatic artificial muscles," in *2011 19th Mediterranean Conference on Control & Automation (MED)*, pp. 1439–1446, IEEE, 2011.

[11] K. Ashwin and A. Ghosal, "A survey on static modeling of miniaturized pneumatic artificial muscles with new model and experimental results," *Applied Mechanics Reviews*, vol. 70, no. 4, p. 040802, 2018.

[12] B. Tondu, "Modelling of the mckibben artificial muscle: A review," *Journal of Intelligent Material Systems and Structures*, vol. 23, no. 3, pp. 225–253, 2012.

[13] S. Krishna, T. Nagarajan, and A. Rani, "Review of current development of pneumatic artificial muscle," *Journal of Applied Sciences*, vol. 11, no. 10, pp. 1749–1755, 2011.

[14] B. Verrelst, R. V. Ham, B. Vanderborght, F. Daerden, D. Lefeber, and J. Vermeulen, "The pneumatic biped "lucy" actuated with pleated pneumatic artificial muscles," *Autonomous Robots*, vol. 18, pp. 201–213, 2005.

[15] N. Saga, T. Nakamura, and K. Yaegashi, "Mathematical model of pneumatic artificial muscle reinforced by straight fibers," *Journal of intelligent material systems and structures*, vol. 18, no. 2, pp. 175–180, 2007.

[16] A. Zhou, G. Shi, and T. Zhong, "Model improvement and experiment validation of pneumatic artificial muscles.," *Chinese Journal of Mechanical Engineering(English Edition)*, vol. 17, no. 1, pp. 36–39, 2004.

[17] N. Saga and T. Saikawa, "Development of a pneumatic artificial muscle based on biomechanical characteristics," *Advanced Robotics*, vol. 22, no. 6-7, pp. 761–770, 2008.

[18] M. S. Xavier, C. D. Tawk, A. Zolfagharian, J. Pinskier, D. Howard, T. Young, J. Lai, S. M. Harrison, Y. K. Yong, M. Bodaghi, *et al.*, "Soft pneumatic actuators: A review of design, fabrication, modeling, sensing, control and applications," *IEEE Access*, vol. 10, pp. 59442–59485, 2022.

[19] A. Al-Ibadi, K. A. Abbas, M. Al-Atwani, and H. Al-Fahaam, "Design, implementation, and kinematics of a twisting robot continuum arm inspired by human forearm movements," *Robotics*, vol. 11, no. 3, p. 55, 2022.

[20] A. Al-Ibadi, "The design and implementation of a single-actuator soft robot arm for lower back pain reduction," *Iraqi J. Electr. Electron. Eng*, no. 3RD, 2020.

[21] S. A. Al-Ibadi, L. A. T. Al Abeach, and M. A. A. Al-Ibadi, "Soft robots: Implementation, modeling, and methods of control," *Indonesian Journal of Electrical Engineering and Informatics (IJEEI)*, vol. 11, no. 1, pp. 194–209, 2023.

[22] Ž. Šitum, S. Herceg, N. Bolf, and Ž. Ujević Andrijić, "Design, construction and control of a manipulator driven by pneumatic artificial muscles," *Sensors*, vol. 23, no. 2, p. 776, 2023.

[23] H. Al-Fahaam, S. Davis, and S. Nefti-Meziani, "The design and mathematical modelling of novel extensor bending pneumatic artificial muscles (ebpams) for soft exoskeletons," *Robotics and Autonomous Systems*, vol. 99, pp. 63–74, 2018.

[24] A. Al-Ibadi, S. Nefti-Meziani, and S. Davis, "Efficient structure-based models for the mckibben contraction pneumatic muscle actuator: The full description of the behaviour of the contraction pma," in *Actuators*, vol. 6, p. 32, MDPI, 2017.

[25] T. Amadeo, D. Van Lewen, T. Janke, T. Ranzani, A. Devaiah, U. Upadhyay, and S. Russo, "Soft robotic deployable origami actuators for neurosurgical brain retraction," *Frontiers in Robotics and AI*, vol. 8, p. 731010, 2022.

[26] W. Al-Mayahi and H. Al-Fahaam, "A novel variable stiffness compound extensor-pneumatic artificial muscle (ce-pam): Design and mathematical model," *Journal of Robotics and Control (JRC)*, vol. 4, no. 3, pp. 342–355, 2023.

[27] A. D. D. R. Carvalho, N. Karanth, and V. Desai, "Characterization of pneumatic muscle actuators and their implementation on an elbow exoskeleton with a novel hinge design," *Sensors and Actuators Reports*, vol. 4, p. 100109, 2022.

[28] H. A. Al-Mosawi, A. Al-Ibadi, and T. Y. Abdalla, "A comprehensive comparison of different control strategies to adjust the length of the soft contractor pneumatic muscle actuator.," *Iraqi Journal for Electrical & Electronic Engineering*, vol. 18, no. 2, 2022.

[29] B. Kalita and S. K. Dwivedy, "Nonlinear dynamic response of pneumatic artificial muscle: A theoretical and experimental study," *International Journal of Non-Linear Mechanics*, vol. 125, p. 103544, 2020.

[30] S. Davis, N. Tsagarakis, J. Canderle, and D. G. Caldwell, "Enhanced modelling and performance in braided pneumatic muscle actuators," *The International Journal of Robotics Research*, vol. 22, no. 3-4, pp. 213–227, 2003.

[31] S. W. Khara, A. Al-Ibadi, H. S. Al-Fahaam, H. El-Hussieny, S. T. Davis, S. Nefti-Meziani, and O. Patrouix, "Compliant pneumatic muscle structures and systems for extra-vehicular and intra-vehicular activities in space environment," 2021.

[32] L. Hines, K. Petersen, G. Z. Lum, and M. Sitti, "Soft actuators for small-scale robotics," *Advanced materials*, vol. 29, no. 13, p. 1603483, 2017.

[33] B. Gorissen, D. Reynaerts, S. Konishi, K. Yoshida, J.-W. Kim, and M. De Volder, "Elastic inflatable actuators for soft robotic applications," *Advanced Materials*, vol. 29, no. 43, p. 1604977, 2017.

[34] H. P. H. Anh, "Online tuning gain scheduling mimo neural pid control of the 2-axes pneumatic artificial muscle (pam) robot arm," *Expert systems with applications*, vol. 37, no. 9, pp. 6547–6560, 2010.

[35] A. Al-Ibadi, S. Nefti-Meziani, and S. Davis, "Design, implementation and modelling of the single and multiple extensor pneumatic muscle actuators," *Systems Science & Control Engineering*, vol. 6, no. 1, pp. 80–89, 2018.

[36] A. Pagoli, F. Chapelle, J.-A. Corrales-Ramon, Y. Mezouar, and Y. Lapusta, "Review of soft fluidic actuators: Classification and materials modeling analysis," *Smart Materials and Structures*, vol. 31, no. 1, p. 013001, 2021.

[37] A. Al-Ibadi, S. Nefti-Meziani, and S. Davis, "Valuable experimental model of contraction pneumatic muscle actuator," in *2016 21st International Conference on Methods and Models in Automation and Robotics (MMAR)*, pp. 744–749, IEEE, 2016.

[38] V. Jouppila, A. Gadsden, and A. Ellman, "Modeling and identification of a pneumatic muscle actuator system controlled by on/off solenoid valve," in *Proceedings of the 7th International Fluid Power Conference IFK, Aachen, Germany, 22-24 March, 2010*, pp. 1–34, 2010.

[39] J. Zuo, Q. Liu, W. Meng, Q. Ai, and S. Q. Xie, "Enhanced compensation control of pneumatic muscle actuator with high-order modified dynamic model," *ISA transactions*, vol. 132, pp. 444–461, 2023.

[40] P. K. Jamwal and S. Q. Xie, "Artificial neural network based dynamic modelling of indigenous pneumatic muscle actuators," in *Proceedings of 2012 IEEE/ASME 8th IEEE/ASME International Conference on Mechatronic and Embedded Systems and Applications*, pp. 190–195, IEEE, 2012.

[41] B. Hannaford and J. Winters, "Actuator properties and movement control: biological and technological models," in *Multiple Muscle Systems: Biomechanics and Movement Organization*, pp. 101–120, Springer, 1990.

[42] G. Klute, J. Czerniecki, and B. Hannaford, "Muscle-like pneumatic actuators for below-knee prostheses," 2000.

[43] B. Kalita and S. Dwivedy, "Dynamic analysis of pneumatic artificial muscle (pam) actuator for rehabilitation with principal parametric resonance condition," *Nonlinear Dynamics*, vol. 97, pp. 2271–2289, 2019.

[44] Ž. Šitum, P. Trslić, D. Trivić, V. Štahan, H. Brezak, and D. Sremić, "Pneumatic muscle actuators within robotic and mechatronic systems," in *Proceedings of International Conference Fluid Power, Fluidna tehnika 2015*, pp. 175–188, Faculty of Mechanical Engineering, 2015.

[45] R. Ranjan, P. Upadhyay, A. Kumar, and P. Dhyani, "Theoretical and experimental modeling of air muscle," *International Journal of Emerging Technology and Advanced Engineering*, vol. 2, no. 4, pp. 112–119, 2012.

[46] S. Kihara, A. Al-Ibadi, H. Al-Fahaam, H. El-Hussieny, S. Davis, S. Nefti-Meziani, and P. Patrouix, "Compliant pneumatic muscle structures and systems for extra-vehicular and intra-vehicular activities in space environments," Institution of Engineering and Technology (IET), 2021.

[47] E. Kelasidi, G. Andrikopoulos, G. Nikolakopoulos, and S. Manesis, "A survey on pneumatic muscle actuators modeling," in *2011 IEEE International Symposium on Industrial Electronics*, pp. 1263–1269, IEEE, 2011.

[48] W. McMahan, V. Chitrakaran, M. Csencsits, D. Dawson, I. D. Walker, B. A. Jones, M. Pritts, D. Dienno, M. Grissom, and C. D. Rahn, "Field trials and testing

of the octarm continuum manipulator," in *Proceedings 2006 IEEE International Conference on Robotics and Automation, 2006. ICRA 2006.*, pp. 2336–2341, IEEE, 2006.

[49] S. Blasiak, J. Takosoglu, and P. Laski, "Optimizing the flow rate in a pneumatic directional control valve," *Eng. Mech*, pp. 96–99, 2014.

[50] J. Bochnia, "Relaxation of materials obtained using polyjet technology," *Engineering Mechanics*, vol. 2017, pp. 178–181, 2017.

[51] H. Al-Fahaam, M. Alaziz, S. Davis, and S. Nefti-Meziani, "Power augmentation and rehabilitation exoskeleton robot based on variable stiffness soft actuators," in *2020 International Conference on Electrical, Communication, and Computer Engineering (ICECCE)*, pp. 1–6, IEEE, 2020.

[52] J. M. Chambers and N. M. Wereley, "Analysis of pneumatic artificial muscles and the inelastic braid assumption," in *Actuators*, vol. 11, p. 219, MDPI, 2022.

[53] N. Tsagarakis and D. G. Caldwell, "Improved modelling and assessment of pneumatic muscle actuators," in *Proceedings 2000 ICRA. Millennium Conference. IEEE International Conference on Robotics and Automation. Symposia Proceedings (Cat. No. 00CH37065)*, vol. 4, pp. 3641–3646, IEEE, 2000.

[54] M. Doumit, A. Fahim, and M. Munro, "Analytical modeling and experimental validation of the braided pneumatic muscle," *IEEE transactions on robotics*, vol. 25, no. 6, pp. 1282–1291, 2009.

[55] R. H. Gaylord, "Fluid actuated motor system and stroking device," July 22 1958. US Patent 2,844,126.

[56] H. F. Schulte, J. R. Pearson, *et al.*, "Characteristics of the braided fluid actuator [by] hf schulte, jr., df adamski [and] jr pearson.," tech. rep., 1961.

[57] H. Schulte, "The characteristics of the mckibben artificial muscle," *The application of external power in prosthetics and orthotics*, pp. 94–115, 1961.

[58] C.-P. Chou and B. Hannaford, "Measurement and modeling of mckibben pneumatic artificial muscles," *IEEE Transactions on robotics and automation*, vol. 12, no. 1, pp. 90–102, 1996.

[59] C.-P. Chou and B. Hannaford, "Static and dynamic characteristics of mckibben pneumatic artificial muscles," in *Proceedings of the 1994 IEEE international conference on robotics and automation*, pp. 281–286, IEEE, 1994.

[60] B. Tondu and P. Lopez, "Modeling and control of mckibben artificial muscle robot actuators," *IEEE control systems Magazine*, vol. 20, no. 2, pp. 15–38, 2000.

[61] D. G. Caldwell, G. A. Medrano-Cerda, and M. Goodwin, "Control of pneumatic muscle actuators," *IEEE Control Systems Magazine*, vol. 15, no. 1, pp. 40–48, 1995.

[62] T. Kimura, S. Hara, T. Fujita, and T. Kagawa, "Feedback linearization for pneumatic actuator systems with static friction," *Control engineering practice*, vol. 5, no. 10, pp. 1385–1394, 1997.

[63] D. G. Caldwell, G. A. Medrano-Cerda, and C. J. Bowler, "Investigation of bipedal robot locomotion using pneumatic muscle actuators," in *Proceedings of International Conference on Robotics and Automation*, vol. 1, pp. 799–804, IEEE, 1997.

[64] S. Davis and D. G. Caldwell, "Braid effects on contractile range and friction modeling in pneumatic muscle actuators," *The International Journal of Robotics Research*, vol. 25, no. 4, pp. 359–369, 2006.

[65] T. Zheng, D. T. Branson, R. Kang, M. Cianchetti, E. Guglielmino, M. Follador, G. A. Medrano-Cerda, I. S. Godage, and D. G. Caldwell, "Dynamic continuum arm model for use with underwater robotic manipulators inspired by octopus vulgaris," in *2012 IEEE international conference on robotics and automation*, pp. 5289–5294, IEEE, 2012.

[66] W. Shen and G. Shi, "An enhanced static mathematical model of braided fibre-reinforced pneumatic artificial muscles," *Proceedings of the Institution of Mechanical Engineers, Part I: Journal of Systems and Control Engineering*, vol. 225, no. 2, pp. 212–225, 2011.

[67] K. Ashwin and A. Ghosal, "A survey on static modeling of miniaturized pneumatic artificial muscles with new model and experimental results," *Applied Mechanics Reviews*, vol. 70, no. 4, p. 040802, 2018.

[68] T. E. Pillsbury, N. M. Wereley, and Q. Guan, "Comparison of contractile and extensile pneumatic artificial muscles," *Smart Materials and Structures*, vol. 26, no. 9, p. 095034, 2017.

[69] A. Al-Ibadi, S. Nefti-Meziani, and S. Davis, "Novel models for the extension pneumatic muscle actuator performances," in *2017 23rd international conference on automation and computing (ICAC)*, pp. 1–6, IEEE, 2017.

[70] W. Najmuddin and M. Mustaffa, "A study on contraction of pneumatic artificial muscle (pam) for load-lifting," in *Journal of Physics: Conference Series*, vol. 908, p. 012036, IOP Publishing, 2017.

[71] X. Li, K. Sun, C. Guo, T. Liu, and H. Liu, "Enhanced static modeling of commercial pneumatic artificial muscles," *Assembly Automation*, vol. 40, no. 3, pp. 407–417, 2020.

[72] S. Ghosh, D. Kumar, and S. Roy, "Static modeling of braided pneumatic muscle actuator: An amended force model," in *AIP Conference Proceedings*, vol. 2584, AIP Publishing, 2023.

[73] H. Zheng and X. Shen, "Double-acting sleeve muscle actuator for bio-robotic systems," in *Actuators*, vol. 2, pp. 129–144, MDPI, 2013.

[74] T. Hassan, M. Cianchetti, B. Mazzolai, C. Laschi, and P. Dario, "A multifunctional pneumatic artificial muscle. proof of concept.," in *15th International Conference on New Actuators & 9th Exhibition on Smart Actuators and Drive SystemsAt: Bremen, Germany*, 2016.

[75] Q. Guan, J. Sun, Y. Liu, N. M. Wereley, and J. Leng, "Novel bending and helical extensile/contractile pneumatic artificial muscles inspired by elephant trunk," *Soft robotics*, vol. 7, no. 5, pp. 597–614, 2020.

[76] M. R. M. Razif, M. Bavandi, I. N. A. M. Nordin, E. Natarajan, O. Yaakob, *et al.*, "Two chambers soft actuator realizing robotic gymnotiform swimmers fin," in *2014 IEEE International Conference on Robotics and Biomimetics (ROBIO 2014)*, pp. 15–20, IEEE, 2014.

[77] B. Mosadegh, P. Polygerinos, C. Keplinger, S. Wennstedt, R. F. Shepherd, U. Gupta, J. Shim, K. Bertoldi, C. J. Walsh, and G. M. Whitesides, "Pneumatic networks for soft robotics that actuate rapidly," *Advanced functional materials*, vol. 24, no. 15, pp. 2163–2170, 2014.

[78] H. Al-Fahaam, S. Davis, S. Nefti-Meziani, and T. Theodoridis, "Novel soft bending actuator-based power augmentation hand exoskeleton controlled by human intention," *Intelligent Service Robotics*, vol. 11, pp. 247–268, 2018.

[79] A.-R. Ziad, M. Al-Ibadi, and A. Al-Ibadi, "Design and implementation of a multiple dof soft robot arm using exestensor muscles," in *2022 9th International Conference on Electrical and Electronics Engineering (ICEEE)*, pp. 170–174, IEEE, 2022.

[80] Y. Chen, J. Zhang, and Y. Gong, "Novel design and modeling of a soft pneumatic actuator based on antagonism mechanism," in *Actuators*, vol. 9, p. 107, MDPI, 2020.

[81] A. Al-Ibadi, S. Nefti-Meziani, and S. Davis, "The design, kinematics and torque analysis of the self-bending soft contraction actuator," in *Actuators*, vol. 9, p. 33, MDPI, 2020.

[82] Q. Guan, J. Sun, Y. Liu, N. M. Wereley, and J. Leng, "Characterization and nonlinear models of bending extensile/contractile pneumatic artificial muscles," *Smart Materials and Structures*, vol. 30, no. 2, p. 025024, 2021.

[83] J.-F. Zhang, C.-J. Yang, Y. Chen, Y. Zhang, and Y.-M. Dong, "Modeling and control of a curved pneumatic muscle actuator for wearable elbow exoskeleton," *Mechatronics*, vol. 18, no. 8, pp. 448–457, 2008.

[84] R. W. Colbrunn, G. M. Nelson, and R. D. Quinn, "Modeling of braided pneumatic actuators for robotic control," in *Proceedings 2001 IEEE/RSJ International Conference on Intelligent Robots and Systems. Expanding the Societal Role of Robotics in the the Next Millennium (Cat. No. 01CH37180)*, vol. 4, pp. 1964–1970, IEEE, 2001.

[85] D. Repperger, K. Johnson, and C. Phillips, "A vsc position tracking system involving a large scale pneumatic muscle actuator," in *Proceedings of the 37th IEEE conference on decision and control (Cat. No. 98CH36171)*, vol. 4, pp. 4302–4307, IEEE, 1998.

[86] J. Serres, D. Reynolds, C. Phillips, M. Gerschutz, and D. Repperger, "Characterisation of a phenomenological model for commercial pneumatic muscle actuators," *Computer Methods in Biomechanics and Biomedical Engineering*, vol. 12, no. 4, pp. 423–430, 2009.

[87] V. Sakthivelu, S.-H. Chong, M. H. Tan, and M. M. Ghazaly, "Phenomenological modeling and classic control of a pneumatic muscle actuator system," *International Journal of Control and Automation*, vol. 9, no. 4, pp. 301–312, 2016.

[88] K. Wickramatunge and T. Leephakpreeda, "Empirical modeling of pneumatic artificial muscle," in *Proceedings of the International MultiConference of Engineers and Computer Scientists*, vol. 2, Citeseer, 2009.

[89] K. C. Wickramatunge and T. Leephakpreeda, "Study on mechanical behaviors of pneumatic artificial muscle," *International Journal of Engineering Science*, vol. 48, no. 2, pp. 188–198, 2010.

[90] M. A. Hoque, E. Petersen, and X. Fang, "Effect of material properties on thin mckibben pneumatic actuators performance," *Available at SSRN 4178077*.